


**AUTHOR QUERY FORM**

 <b>ELSEVIER</b>	<b>Journal:</b> RM	<b>Please e-mail or fax your responses and any corrections to:</b>
	<b>Article Number:</b> 4009	<b>E-mail:</b> <a href="mailto:corrections.esch@elsevier.tnq.co.in">corrections.esch@elsevier.tnq.co.in</a> <b>Fax:</b> +31 2048 52789

Dear Author,

Any queries or remarks that have arisen during the processing of your manuscript are listed below and highlighted by flags in the proof. Please check your proof carefully and mark all corrections at the appropriate place in the proof (e.g., by using on-screen annotation in the PDF file) or compile them in a separate list.

For correction or revision of any artwork, please consult <http://www.elsevier.com/artworkinstructions>.

**Articles in Special Issues:** Please ensure that the words ‘this issue’ are added (in the list and text) to any references to other articles in this Special Issue.

<b>Uncited references:</b> References that occur in the reference list but not in the text – please position each reference in the text or delete it from the list.	
<b>Missing references:</b> References listed below were noted in the text but are missing from the reference list – please make the list complete or remove the references from the text.	
Location in article	Query / remark Please insert your reply or correction at the corresponding line in the proof
<b>Q1</b>	Reference list mentions “Ogorodnikov et al., 2002a” and “2002b” as separate references. Therefore we have changed all citations of “Ogorodnikov et al., 2002” to “Ogorodnikov et al., 2002a,b”. Please amend the text citations as appropriate.
<b>Q2</b>	Please note that “ $\omega_0 = 4 \times 10^5 \text{ s}^{-1}$ ” in the sentence “An analysis revealed that...” has been changed to “ $\omega_0 = 4 \times 10^5 \text{ s}^{-1}$ ”, kindly check.

**Electronic file usage**

Sometimes we are unable to process the electronic file of your article and/or artwork. If this is the case, we have proceeded by:

Scanning (parts of) your article

Rekeying (parts of) your article

Scanning the artwork

Thank you for your assistance.



Contents lists available at ScienceDirect

## Radiation Measurements

journal homepage: [www.elsevier.com/locate/radmeas](http://www.elsevier.com/locate/radmeas)Short-living defects and recombination processes in  $\text{Li}_6\text{Gd}(\text{BO}_3)_3$  crystalsI.N. Ogorodnikov<sup>a,\*</sup>, N.E. Poryvay<sup>a</sup>, V.A. Pustovarov<sup>a</sup>, A.V. Tolmachev<sup>b</sup>, R.P. Yavetskiy<sup>b</sup>, V.Yu. Yakovlev<sup>c</sup><sup>a</sup> Experimental Physics Department, Ural State Technical University, Mira Street, 19, Ekaterinburg 620002, Russia<sup>b</sup> STC Institute for Single Crystals NAS of Ukraine, Lenin ave., 60, Kharkov 61001, Ukraine<sup>c</sup> Tomsk Polytechnic University, Lenin ave., 30, Tomsk 634050, Russia

## ARTICLE INFO

## Article history:

Received 23 July 2009

Received in revised form

9 December 2009

Accepted 28 January 2010

## Keywords:

Optical spectroscopy

Time-resolution

Lattice defects

Lithium borate crystals

 $\text{Li}_6\text{Gd}(\text{BO}_3)_3$ 

## ABSTRACT

Results of a study of transient optical absorption (TOA) and luminescence of lithium-gadolinium orthoborate  $\text{Li}_6\text{Gd}(\text{BO}_3)_3$  (LGBO) in the visible and ultraviolet spectral regions are presented. As revealed by absorption optical spectroscopy with nanosecond time resolution, the LGBO TOA derives from optical transitions in hole centers, with the optical density relaxation kinetics being mediated by interdefect tunneling recombination involving these centers and neutral lithium atoms acting as electronic  $\text{Li}^0$  centers. At 290 K, the  $\text{Li}^0$  centers are involved in thermally stimulated migration, which is not accompanied by carrier transfer to the conduction or valence band. The slow TOA decay kinetics components, with characteristic times ranging from a few milliseconds to seconds, have been assigned to diffusion-limited annihilation of lithium interstitials with vacancies. The mechanisms responsible for the creation and relaxation of short-living Frenkel defect pairs in the LGBO cation sublattice have been analyzed.

© 2010 Published by Elsevier Ltd.

## 1. Introduction

Crystalline borates of alkali and alkaline-earth metals form a broad class of wide-bandgap oxide dielectrics which have been attracting considerable interest in the recent years, both in basic science and in the field of applications as detector, conversion and waveguide optical media intended for operation in the ultraviolet and vacuum ultraviolet spectral regions (Chen et al., 1989). These compounds share a number of common properties. Among them are the low crystal symmetry, an intricate lattice cell and the existence both of pure covalent chemical bonding within the boron-oxygen anion groups and of comparatively weak ionic bonds coupling the cation with the corresponding anion group.

A sublattice of weakly bonded cations combined with a stable boron-oxygen framework should affect strongly the dynamics of electronic excitations and characteristic features of radiation-induced defect formation. This problem becomes particularly acute in the case of lightweight mobile small-radius cations, for instance, in lithium borate crystals. In our previous research works, this aspect was studied in the particular example of crystals with a lattice of mobile lithium cations ( $\text{Li}_2\text{B}_4\text{O}_7$  (Ogorodnikov et al., 2002a,b),  $\text{LiB}_3\text{O}_5$  (Ogorodnikov et al., 2003)) and model dihydrophosphates with a sublattice of mobile hydrogen cations ( $\text{NH}_4\text{H}_2\text{PO}_4$  and  $\text{KH}_2\text{PO}_4$  (Ogorodnikov et al., 2002a)).

Single crystals of the lithium-gadolinium orthoborate LGBO ( $\text{Li}_6\text{Gd}(\text{BO}_3)_3$ ) are in this respect of particular significance, primarily as a promising optical material for neutron detection by the scintillation technique (Czirr et al., 1999; van Eijk, 2004).

The main goal of the present work is a study of the processes involved in the creation and evolution of short-living radiation-induced defects on the cation sublattice of LGBO crystals by the means of the time-resolved luminescence and optical spectroscopy under excitation by a nanosecond-scale pulsed electron beam.

## 2. Experimental details

We used lithium-gadolinium borate crystals, both undoped (LGBO) and cerium-doped (LGBO-Ce). The samples were plane-parallel transparent plates measuring  $6 \times 5 \times 1 \text{ mm}^3$ . The crystals were grown at the Institute of Single Crystals, National Academy of Sciences of Ukraine (Kharkov), by the Czochralski method in the air atmosphere (Baumer et al., 2002).

The experimental setup and the main characteristics of the luminescence and absorption spectroscopy with a nanosecond-scale time-resolution employed are described in considerable details in Yakovlev (1992).

## 3. Results and discussion

Excitation of LGBO crystals with a single nanosecond-range electron pulse brought about a short drop in optical transparency

\* Corresponding author. Tel.: +7 343 3754711; fax: +7 343 3744391.

E-mail address: [igor.ogorodnikov@bk.ru](mailto:igor.ogorodnikov@bk.ru) (I.N. Ogorodnikov).

of the crystal, i.e., an induced transient optical absorption event (TOA). The decay time of this absorption exceeds by many orders of magnitude the length of the exciting electron beam pulse. The broad (not unfolded) TOA spectrum (Fig. 1) is located in the region of optical transparency of the crystal.

Fig. 2 plots the kinetics of TOA decay measured at  $h\nu = 3.7$  eV and 100% excitation power. An analysis of the kinetics revealed that while at  $T = 290$  K slow monotonic relaxation of induced optical density occurs within a broad (9 decades) time interval, the dynamic range of its variation is relatively small.

One could isolate two decay-time regions differing in the decay pattern. In the micro- and millisecond region, experimental curves allow readily rectification within 3–4 decay time decades when plotted in log–log coordinates (Fig. 2).

They can formally be described by the relation

$$-\log D(t) = A + p \cdot \log t. \quad (1)$$

The exponent  $p$  depends on decay time and lies within 0.04–0.20. Such properties are characteristic of interdefect tunneling recombination kinetics. In the case where the concentration of one of the recombination partners  $N$  exceeds by far that of defects of another species  $n$  which account for the observed TOA, one can write the equation of Parmon et al. (1974)

$$n(t) = n_0 \exp\left(-\frac{4}{3}\pi a^3 N \ln^3(\nu_0 t)\right), \quad (2)$$

where  $\nu_0$  is the prefactor, and  $a$  is one half of the Bohr radius, the parameters which determine the electron tunneling transfer probability  $W$ .

For long decay times, the TOA kinetics also follows the straight line (1) but with an exponent  $p = 1$ , which assumes a first-order hyperbolic relation

$$D(t) = \frac{D_h}{1 + t/t_h}, \quad (3)$$

where  $D_h$  is the optical density corresponding to the initial concentration of the color centers accounting for the given TOA decay kinetics component, and  $t_h$  is the characteristic half-life time of these defects. Fig. 2 plots the results of approximation of the LGBO TOA decay kinetics in the 3.7 eV band with a sum of relations (2) and (3) for decay times extending over about nine decades.

An increase of excitation pulse power gives rise to an increase of the initial concentration of the radiation defects created by this pulse. This brings about a certain “shortening” of the TOA decay kinetics. When plotted in log–log coordinates, the initial optical density  $D(0)$ , which is proportional to the initial concentration of

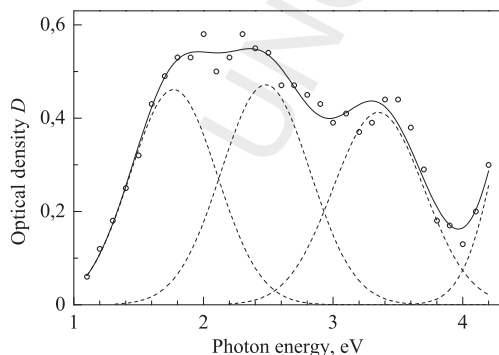


Fig. 1. TOA spectrum of LGBO crystals measured at  $T = 290$  K. Dashed lines plot the main deconvoluted Gaussian bands, symbols relate to experimental data, and the solid line is the result of approximation.

radiation defects, grows by a linear law with a slope close to unity throughout the spectral range covered (Fig. 3). This may suggest the non-impurity nature of the LGBO color centers and a common mechanism of breakup of the radiation defects accounting for the different LGBO TOA bands.

Heating of the crystal likewise brings about “shortening” of the TOA decay kinetics, but the initial optical density  $D(0)$  does not exhibit here any noticeable changes. Both TOA decay kinetics components in the 1.0–4.0 eV region exhibit the same behavior with temperature. Fig. 4 shows the temperature dependence of the time constant  $t_h$  for the hyperbolic component of the TOA decay kinetics. An analysis revealed that  $1/t_h(T)$  obeys the Arrhenius law with a thermal activation energy  $E_a = 0.32$  eV and a prefactor  $\omega_0 = 4 \times 10^5 \text{ s}^{-1}$

$$\frac{1}{t_h(T)} = \omega_0 \cdot \exp\left(-\frac{E_a}{k_b T}\right), \quad (4)$$

where  $k_b$  is the Boltzmann constant.

Electron beam excitation of an LGBO crystal at  $T = 290$  K initiates also pulsed cathodoluminescence (PCL) in the 2.5–3.5 eV region with a characteristic decay time comparable with the length of the excitation pulse. The observed signal is in this case actually a Gaussian excitation pulse ( $\tau = 12$  ns) convolved with the PCL decay kinetics of the sample. A numerical analysis of the experimental data suggests that the PCL decay kinetics in the band at 3.0 eV is dominated in intensity by an exponential component with a time constant  $\tau = 45$  ns accompanied by slow and weak components of the micro- and millisecond ranges. Fig. 5 displays the slow PCL decay kinetics components measured within a luminescence intensity variation range extending over about 3.5 decades.

The main contribution to the PCL decay kinetics derives in this time range from a slow component obeying the relation  $I(t) \propto 1/t$ . The second slow component can be fitted by a second-order hyperbolic relation with a time constant of 120  $\mu\text{s}$  at  $T = 290$  K and an initial intensity of about 3% of the maximum PCL intensity.

Fig. 6 presents a pulsed cathodoluminescence spectrum based on the amplitudes of observed signals (oscillograms), which were measured at termination of the excitation pulse. As evident from Fig. 6, the PCL spectrum of a LGBO crystal represents essentially a composite band covering the 2.5–3.5 eV interval. The intensity of this PCL band is higher in LGBO crystals doped by  $\text{Ce}^{3+}$  ions. This may be considered as an indirect indication of the color centers accounting for this PCL band being of the impurity nature.

To provide a basis for discussion of the nature of the radiation defects formed, compare the characteristic features of the TOA (Fig. 1) we found with known optical spectroscopy data for the LGBO crystals. The starting undoped LGBO crystals are optically transparent in the spectral region of up to 3.9 eV. At 4.4–5.2 eV one can see groups of optical absorption lines corresponding to transitions from the  $^8S_{7/2}$  ground state of the  $\text{Gd}^{3+}$  ion to its  $^6D_j$  and  $^6I_j$  excited states Garapon et al. (1985). Doping with cerium brings about the appearance in the spectrum of steady-state optical absorption of LGBO-Ce crystals maxima in the 3.54 and 3.88 eV regions which correspond to the  $4f$ – $5d$  transitions in  $\text{Ce}^{3+}$  ions. One observes also a composite band at 4.1 eV deriving from charge transfer transitions, i.e., electron transfer from the  $2p$  oxygen orbital to the empty  $4f$  orbital of the cerium ion.

Yavetskiy et al. (2007) established that following  $\beta$  irradiation, spectra of steady-state optical absorption of LGBO and LGBO-Eu exhibit enhancement of the amplitude of the band at 3.25 eV, which was attributed to the absorption of  $\text{O}^-$  centers coupled with lithium growth vacancies.

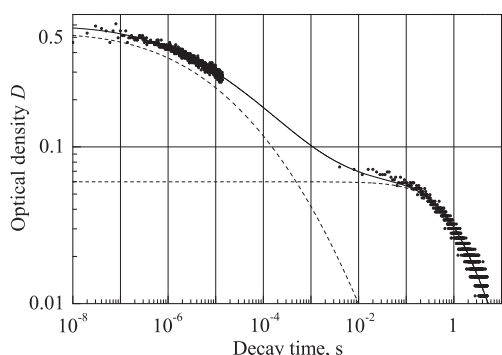


**Fig. 2.** TOA decay kinetics of LGBO crystals in the 3.7 eV band.  $T = 290$  K. Dashed lines show components of the decay kinetics, symbols are experimental data, and the solid line is the result of approximation.

The properties of the transient optical absorption observed by us in the 1.0–4.0 eV region (Fig. 1) can not be correlated with the above data on the optical spectroscopy of LGBO and LGBO-Ce. All the more so that available data bear only on steady-state optical absorption bands which are stable at room temperature.

We believe that the nature of the observed TOA should rather be attributed to formation in a LGBO crystal of short-living radiation defects induced by the electron beam. An analysis of the crystallographic structure of LGBO suggests that the most probable effect of the action of an electron beam is creation of Frenkel defect pairs on the sublattice of weakly bound lithium cations, namely, of an interstitial lithium ion and a cation lithium vacancy. Subsequent trapping of the band electron by the lithium ion may result in formation of the  $\text{Li}^0$  electronic center, while trapping a band hole into  $2p$  orbitals of one of the oxygen ions surrounding a lithium vacancy gives rise to formation of an  $\text{O}^-$  type hole center. Such mechanism of radiation defect formation was observed by us earlier to realize in  $\text{Li}_2\text{B}_4\text{O}_7$  (Ogorodnikov et al., 2002a,b) and  $\text{LiB}_3\text{O}_5$  (Ogorodnikov et al., 2003) lithium borate crystals.

The broad optical absorption bands of hole centers in oxides are usually assigned to optical transitions between valence band states of the crystal and a local level of the hole center. It is known that the  $\text{O } 2p$ - and  $\text{B } 2p$ -like hybridized states provide a major contribution to valence band top states of the borates, while levels of the conduction band bottom derive from  $d$ -states of metals. In the vicinity of a cation vacancy in oxides, valence band top states become usually split off into the bandgap. Therefore, we are inclined to associate the mechanism of transient optical absorption in LGBO crystals with photoinduced hole transfer between the  $2p$

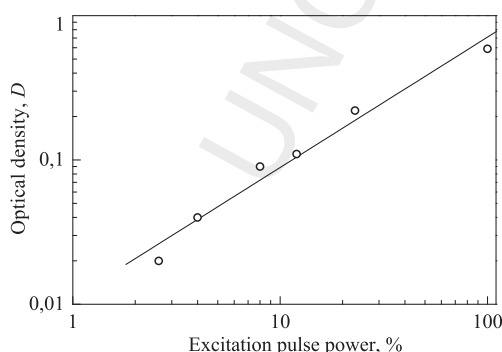


**Fig. 3.** Optical density in the 3.8 eV band measured immediately after termination of the excitation pulse and plotted vs. electron beam power (percents of the maximum power) for a LGBO crystal.  $T = 290$  K. Symbols are experimental data, and the straight line is the approximation.

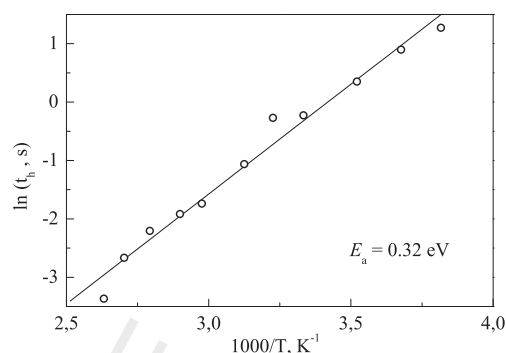


**Fig. 4.** Temperature dependence of the TOA decay kinetics parameter  $t_h$  of a LGBO crystal in the 3.7 eV band. Symbols are experimental data, and the straight line is the approximation.

states of neighboring anions surrounding a lithium vacancy. Considered in the context of the theory of small-radius polarons, this process is treated as inter-polaron absorption. The profile of the optical absorption spectrum is largely mediated in these conditions by the distribution of the density of valence band states. At  $T = 290$  K, a hole undergoes thermally activated and, possibly, partially tunneling migration among the anions surrounding the vacancy. The energy threshold of optical absorption (1.2 eV in Fig. 1) is actually the energy of an optical transition between the local level of the hole center and the valence band top, i.e., the optical activation energy of the  $\text{O}^-$  hole center. Optical absorption of this type was observed by us earlier in the  $\text{Li}_2\text{B}_4\text{O}_7$  (Ogorodnikov et al., 2002a,b) and  $\text{LiB}_3\text{O}_5$  (Ogorodnikov et al., 2003) lithium borate crystals.

The concentration of the  $\text{O}^-$  centers responsible for the TOA can decrease not only through the ionic process of diffusion-limited annihilation of lithium vacancies with  $\text{Li}^0$  interstitial atoms, but in tunneling charge exchange of these defects involving tunneling transfer of an electron from the interstitial  $\text{Li}^0$  atom to the  $\text{O}^-$  center as well. It is this transfer that accounts for the main ‘tunneling component’ in the LGBO TOA decay kinetics. This appears to provide reasonable grounds for the use of the theory of tunneling charge exchange among randomly distributed defects and for fitting Eq. (2) to the TOA kinetics in describing the above component. The probability of tunneling electron transfer between the tunneling recombination partners depends on the prefactor  $\nu_0$  and distance  $r$  between the partners. The lithium cation mobility affects the distribution of defect pairs in defect separations  $r$  and gives rise to an increase in the ‘close pair’ concentration. This accounts for the

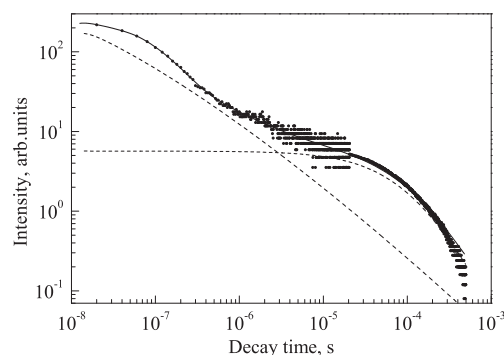


**Fig. 5.** Slow components of LGBO PCL decay kinetics in the 3.0 eV band.  $T = 290$  K. Dashed lines indicate the decay kinetics components, symbols are experimental data, and the solid line is the approximation.

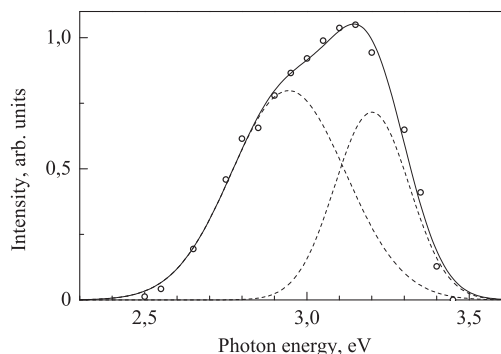


**Fig. 6.** PCL spectrum of LGBO crystals obtained at  $T = 290$  K. Dashed lines plot the main Gaussian constituents, symbols are experimental data, and the straight line is the approximation.

observed temperature dependence of the ‘tunneling’ component of the TOA decay kinetics. We observed a similar temperature dependence of the ‘tunneling’ TOA decay kinetics component in an earlier study of the  $\text{Li}_2\text{B}_4\text{O}_7$  (Ogorodnikov et al., 2002a,b) and  $\text{LiB}_3\text{O}_5$  (Ogorodnikov et al., 2003) lithium borate crystals.

The hole color centers responsible for the TOA are intrinsic LGBO lattice defects, whose concentration plotted in log–log coordinates grows linearly with increasing excitation pulse power by nearly two orders of magnitude. As follows directly from Eq. (2), the decay kinetics of both TOA components should shorten with increasing initial concentration of radiation defects. It is exactly this pattern that we observed in the experiment.

A comprehensive comparison of the TOA (Fig. 2) and PCL (Fig. 5) decay patterns suggests that the decay kinetics of the first slow PCL component can be fitted by a time derivative of the ‘tunneling’ component of the TOA decay kinetics. Eq. (2) shows readily that

$$I(t) = -\frac{dn}{dt} = \frac{4}{3}\pi a^3 N \cdot n(t) \cdot \frac{\ln^2(v_0 t)}{t}. \quad (5)$$

This implies that tunneling electron transfer between the tunneling recombination partners accounting for the TOA kinetics is radiative, and that this tunneling transfer of an electron from a defect to the excited state of the color center occurs in resonant (or close to resonant) conditions. It appears reasonable to maintain that the ‘tunneling’ component of the TOA decay kinetics and the first slow component in the PCL decay kinetics are mediated by the same relaxation process.

At the same time, the fast and the second slow components in PCL decay and the TOA decay kinetics in LGBO are not related and are mediated by different relaxation processes. The main PCL band of LGBO-Ce at 3.0–3.1 eV (Fig. 6) can be identified in its spectral and kinetics characteristics with the well-known luminescence band of  $\text{Ce}^{3+}$ . We believe that excitation with an electron beam gives rise to ionization of the  $\text{Ce}^{3+}$  impurity center involving electron transfer to the conduction band,  $\text{Ce}^{3+} \rightarrow e^- + \text{Ce}^{4+}$ . In relaxation, the band electron becomes trapped in the excited  $5d$  state of the  $\text{Ce}^{3+}$  ion, with subsequent luminescence in the 3.0–3.1 eV band:  $e^- + \text{Ce}^{4+} \rightarrow (\text{Ce}^{3+})^* \rightarrow \text{Ce}^{3+} + h\nu$ . On termination of the excitation pulse, the luminescence decays. Because of the presence of shallow

band-electron trapping centers, the decay time constant of the recombination luminescence ( $\tau = 45$  ns) exceeds slightly the radiative lifetime of the  $\text{Ce}^{3+}$  luminescence center. The luminescence decay time constant of the  $\text{Ce}^{3+}$  centers in the case of a direct photoexcitation is  $\tau_r = 28$  ns. This mechanism of  $\text{Ce}^{3+}$  luminescence is fairly universal; for the case of X-rays excitation it was considered to realize in a number of crystals, in particular, in borates, and for LGBO-Ce it was analyzed earlier by us in (Ogorodnikov et al., 2007).

#### 4. Conclusions

To sum up, we have carried out the first investigation of the formation and evolution of short-living radiation-induced defects on the cation sublattice in LGBO crystals by time-resolved luminescence and optical spectroscopy under a nanosecond time-range electron beam excitation. The analysis performed has permitted identification of the mechanism responsible for the creation and relaxation of short-living Frenkel defect pairs on the LGBO cation sublattice. By the concept developed, the observed transient optical absorption in LGBO derives from photoinduced hole transfer between  $2p$  states of neighboring anions surrounding the lithium vacancy, and TOA decay kinetics is mediated primarily by tunneling electron transfer between the intrinsic lattice defects, namely, the electronic  $\text{Li}^0$  and the hole  $\text{O}^-$  centers. This mechanism of radiation-induced defect formation appears fairly universal for crystals with the sublattice of mobile lithium cations. Similar results were obtained earlier in our studies of some other lithium-containing crystals,  $\text{Li}_2\text{B}_4\text{O}_7$  (Ogorodnikov et al., 2002a,b) and  $\text{LiB}_3\text{O}_5$  (Ogorodnikov et al., 2003).

#### References

- Baumer, V.N., Grinyov, B.V., Dubovik, M.F., Dolzhenkova, E.F., Korshikova, T.I., Tolmachev, A.V., Shekhovtsov, A.N., 2002. Study of peculiarities of the growth process and crystal structure of single crystals  $\text{Li}_6\text{Gd}(\text{BO}_3)_3$ . *Poverkhnost* 5, 62–64.
- Chen, C., Wu, Y., Jaing, A., Wu, B., You, G., Lin, S., 1989. New nonlinear-optical crystal:  $\text{LiB}_3\text{O}_5$ . *J. Opt. Soc. Am. B* 6, 616–621.
- Cziri, J.B., MacGillivray, G.M., MacGillivray, R.R., Seddon, P.J., 1999. Performance and characteristics of a new scintillator. *Nucl. Instrum. Methods Phys. Res., Sect. A* 424, 15–19.
- van Eijk, C.W.E., 2004. Inorganic scintillators for thermal neutron detection. *Radiat. Meas.* 38, 337–342.
- Garapon, C.T., Jacquier, B., Chaminade, J.P., Fouassier, C., 1985. Energy transfer in  $\text{Li}_6\text{Gd}(\text{BO}_3)_3$ . *J. Lumin.* 34, 211–222.
- Ogorodnikov, I.N., Yakovlev, V.Yu., Kruzhalov, A.V., Isaenko, L.I., 2002a. Transient optical absorption and luminescence in  $\text{Li}_2\text{B}_4\text{O}_7$  lithium tetraborate. *Phys. Solid State* 44, 1085–1092.
- Ogorodnikov, I.N., Yakovlev, V.Yu., Shul'gin, B.V., Satybaldieva, M.K., 2002b. Transient optical absorption of hole polarons in ADP ( $\text{NH}_4\text{H}_2\text{PO}_4$ ) and KDP ( $\text{KH}_2\text{PO}_4$ ) crystals. *Phys. Solid State* 44, 880–887.
- Ogorodnikov, I.N., Yakovlev, V.Yu., Isaenko, L.I., 2003. Transient optical absorption and luminescence of lithium triborate  $\text{LiB}_3\text{O}_5$ . *Phys. Solid State* 45, 845–853.
- Ogorodnikov, I.N., Pustovarov, V.A., Omelkov, S.I., Tolmachev, A.V., Yavetskiy, R.P., 2007. Luminescence VUV spectroscopy of cerium- and europium-doped lithium borate crystals. *Opt. Spectrosc.* 102, 60–67.
- Parmon, V.N., Khairutdinov, R.F., Zamaraev, K.I., 1974. Formal kinetics of tunneling electron transfer in solids. *Sov. Phys. Solid State* 16, 1672–1675.
- Yakovlev, V.Yu., 1992. Time-resolved optical spectroscopy of CsCl crystals subjected to cascade pulsed excitation. *Sov. Phys. Solid State* 34, 651–654.
- Yavetskiy, R.P., Tolmachev, A.V., Dolzhenkova, E.F., Baumer, V.N., 2007. Thermally stimulated luminescence mechanism of  $\text{Li}_6\text{Y}(\text{BO}_3)_3:\text{Eu}^{3+}$  single crystals. *J. Alloys Compd.* 429, 77–81.